Shape-Selective Sorption and Fluorescence Sensing of Aromatics in a Flexible Network of Tetrakis[(4-methylthiophenyl)ethynyl]silane and $AgBF_4$

Guo Huang,[†] Chen Yang,[†] Zhengtao Xu,*[,†] Haohan Wu,[‡] Jing Li,[‡] Matthias Zeller,[§] Allen D. Hunter,[§] Stephen Sin-Yin Chui,[||] and Chi-Ming Che[||]

Department of Biology and Chemistry, City University of Hong Kong, 83 Tat Chee Avenue, Kowloon, Hong Kong, P. R. China, Department of Chemistry & Chemical Biology, Rutgers University, 610 Taylor Road, Piscataway, New Jersey 08854, Department of Chemistry, Youngstown State University, One University Plaza, Youngstown, Ohio 44555, and Department of Chemistry and HKU-CAS Joint Laboratory on New Materials, The University of Hong Kong, Pokfulam Road, Hong Kong, China

Received October 11, 2008. Revised Manuscript Received November 30, 2008

The large tetrapod tetrakis[(4-methylthiophenyl)ethynyl]silane was crystallized with $AgBF_4$ to form a diamondoid network based on the Ag(I)−thioether interaction. A 4-fold interpenetration of the individual nets was observed, with the rest of the unit-cell volume occupied by the benzene guests. The benzene molecules can be removed without collapsing of the host networks, even though the benzene molecules appear to be well enclathrated in the cavities formed by the host nets. Interestingly, the apohost displays a strict size selectivity for small aromatic molecules, which effectively excludes ortho- and meta-substituted benzene derivatives from entering the pores, enabling, for example, the selective sorption of benzene over hexafluorobenzene. The fluorescence arising from the molecular building block also provides for the sensing of nitrobenzene molecules, which effectively quenches the fluorescence upon entry into the host net.

Introduction

Separation and fluorescence sensing of guest species represent two major potential applications for crystalline coordination networks.[1−6] Examples of sorption studies in crystalline coordination networks include selective binding of alcohol molecules,[7,8] separating alkane molecules of different shapes and sizes,[9,10] and small aromatics,[11−14] whereas the capability of fluorescence sensing can be derived from the polarizable organic-based π-electron systems[15,16] or metal-centered emission (preferably with open metal sites).[17,18] Recently, structural dynamics and flexibility of the host network in the context of sorption behaviors have received increasing attention.[3–5,11,14,19−21] In these dynamic systems, the diffusion of guest species is often accompanied by significant structural changes in the host networks, which often significantly modifies the guest transport process.

In a related project, our group endeavors to integrate large aromatic molecules into coordination networks.[22−26] Besides the intense photophysical properties (e.g., photoluminescence) generally associated with the conjugated aromatic π systems, the large size of the organic molecules may in some cases help enhance the structural flexibility of the resultant

* Corresponding author. E-mail: zhengtao@cityu.edu.hk.
[†] City University of Hong Kong.
[‡] Rutgers University.
[§] Youngstown State University.
[||] The University of Hong Kong.

(1) Férey, G. *Chem. Soc. Rev.* **2008**, *37*, 191.
(2) Kitagawa, S.; Kitaura, R.; Noro, S.-i. *Angew. Chem., Int. Ed.* **2004**, *43*, 2334.
(3) Tanaka, D.; Kitagawa, S. *Chem. Mater.* **2008**, *20*, 922.
(4) Bradshaw, D.; Claridge, J. B.; Cussen, E. J.; Prior, T. J.; Rosseinsky, M. J. *Acc. Chem. Res.* **2005**, *38*, 273.
(5) Kepert, C. J. *Chem. Commun.* **2006**, 695.
(6) Dalgarno, S. J.; Thallapally, P. K.; Barbour, L. J.; Atwood, J. L. *Chem. Soc. Rev.* **2007**, *36*, 236.
(7) Pan, L.; Parker, B.; Huang, X.; Olson, D. H.; Lee, J.; Li, J. *J. Am. Chem. Soc.* **2006**, *128*, 4180.
(8) Yaghi, O. M.; Davis, C. E.; Li, G. M.; Li, H. L. *J. Am. Chem. Soc.* **1997**, *119*, 2861.
(9) Pan, L.; Olson, D. H.; Ciemnolonski, L. R.; Heddy, R.; Li, J. *Angew. Chem., Int. Ed.* **2006**, *45*, 616.
(10) Chen, B.; Liang, C.; Yang, J.; Contreras, D. S.; Clancy, Y. L.; Lobkovsky, E. B.; Yaghi, O. M.; Dai, S. *Angew. Chem., Int. Ed.* **2006**, *45*, 1390.
(11) Zhang, J.-P.; Chen, X.-M. *J. Am. Chem. Soc.* **2008**, *130*, 6010.
(12) Finsy, V.; Verelst, H.; Alaerts, L.; De Vos, D.; Jacobs, P. A.; Baron, G. V.; Denayer, J. F. M. *J. Am. Chem. Soc.* **2008**, *130*, 7110.
(13) Choi, E.-Y.; Park, K.; Yang, C.-M.; Kim, H.; Son, J.-H.; Lee, S. W.; Lee, Y. H.; Min, D.; Kwon, Y.-U. *Chem.—Eur. J.* **2004**, *10*, 5535.
(14) Biradha, K.; Hongo, Y.; Fujita, M. *Angew. Chem., Int. Ed.* **2002**, *41*, 3395.
(15) Pang, J.; Marcotte, E. J. P.; Seward, C.; Brown, R. S.; Wang, S. *Angew. Chem., Int. Ed.* **2001**, *40*, 4042.
(16) Das, S.; Bharadwaj, P. K. *Inorg. Chem.* **2006**, *45*, 5257.
(17) Chen, B.; Yang, Y.; Zapata, F.; Lin, G.; Qian, G.; Lobkovsky, E. B. *Adv. Mater.* **2007**, *19*, 1693.
(18) Chen, B.; Wang, L.; Zapata, F.; Qian, G.; Lobkovsky, E. B. *J. Am. Chem. Soc.* **2008**, *130*, 6718.
(19) Kepert, C. J.; Prior, T. J.; Rosseinsky, M. J. *J. Am. Chem. Soc.* **2000**, *122*, 5158.
(20) Bradshaw, D.; Prior, T. J.; Cussen, E. J.; Claridge, J. B.; Rosseinsky, M. J. *J. Am. Chem. Soc.* **2004**, *126*, 6106.
(21) Kawano, M.; Fujita, M. *Coord. Chem. Rev.* **2007**, *251*, 2592.
(22) Sun, Y.-Q.; Tsang, C.-K.; Xu, Z.; Huang, G.; He, J.; Zhou, X.-P.; Zeller, M.; Hunter, A. D. *Cryst. Growth Des.* **2008**, *8*, 1468.
(23) Huang, G.; Xu, H.; Zhou, X.-P.; Xu, Z.; Li, K.; Zeller, M.; Hunter, A. D. *Cryst. Growth Des.* **2007**, *7*, 2542.
(24) Sun, Y.-Q.; He, J.; Xu, Z.; Huang, G.; Zhou, X.-P.; Zeller, M.; Hunter, A. D. *Chem. Commun.* **2007**, 4779.
(25) Li, K.; Huang, G.; Xu, Z.; Carroll, P. J. *J. Solid State Chem.* **2006**, *179*, 3688.
(26) Li, K.; Xu, Z.; Xu, H.; Carroll, P. J.; Fettinger, J. C. *Inorg. Chem.* **2006**, *45*, 1032.

10.1021/cm8027687 CCC: $40.75
Published on Web 01/06/2009

Scheme 1[a]

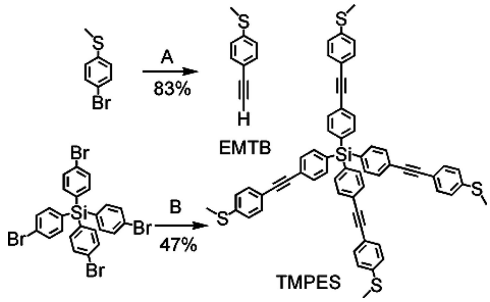

[a] Reagents and conditions: (A) TMSA, $Pd(PPh_3)_2Cl_2$, PPh_3, CuI, triethylamine/THF, 90 °C; TBAF, THF, rt; (B) EMTB, *n*-butyllithium, $ZnCl_2$, THF, −78 °C; $Pd(PPh_3)_4$, toluene, 120 °C.

networks. As such an example, we here report on the remarkable sorption and sensing properties of a coordination network based on the tetrapod-like molecule tetrakis[(4-methylthiophenyl)ethynyl]silane (TMPES, see Scheme 1), which features long and slender branches that might contribute to the structural flexibility observed.

The network features an overall composition of $TMPES \cdot AgBF_4 \cdot 3C_6H_6$ (henceforth called **1**), and displays strict size selectivity for the sieving of small aromatic molecules, enabling a wide range of selective sorption properties, including the ability to separate benzene from hexafluorobenzene (HFB). Moreover, the distinct fluorescence arising from the large conjugated π systems of the molecular building unit can be selectively quenched by nitrobenzene molecules, pointing to its potential use as a solid-state sensor for nitrobenzene. On the fundamental side, this discovery also serves to highlight the structural and functional flexibility that could potentially be achieved from a large aromatic building unit such as TMPES.

Experimental Section

General Procedure. Starting materials, reagents, and solvents were purchased from commercial sources (Aldrich and Fisher Scientific) and used without further purification unless stated otherwise. Solution ^1H and ^{13}C NMR spectra were recorded on a 300 MHz Varian YH300 superconducting-magnet high-field NMR spectrometer at room temperature, with tetramethylsilane (TMS) as the internal standard. Single-crystal XRD analyses (data collection, structure solution and refinement) were carried out at 100(2) K on a Bruker AXS SMART APEX CCD system using Mo Kα (λ = 0.71073 Å) radiation. The structures were solved and refined by full-matrix least-squares on F_o^2 using SHELXL 6.14. X-ray diffraction patterns for the bulk samples in Figure 1 were collected in capillary transmission mode on a Bruker D8 Advance diffractometer equipped with a Göbel mirror that produces parallel X-ray radiation (Cu Kα, λ = 1.5418 Å). The power of the sealed X-ray tube was 40 kV and 40 mA. X-ray diffraction patterns for the bulk samples in Figure S3 in the Supporting Information were collected in reflection mode at room temperature on a Siemens D500 (Cu Kα, λ = 1.5418 Å). The powder samples were pressed onto a glass slide for data collection (in air). Elemental analysis was performed with a Vario EL III CHNOS elemental analyzer. Luminescence spectra were measured using a Horiba Jobin Yvon FL-1057 spectrofluorometer. Thermogravimetric analysis (TGA) was carried out on a Pyris TGA-1 instrument under flowing He gas (20 mL/min) and a heating rate of 5 °C/min. The simulation was done using Cerius2 developed by Accelrys Inc.

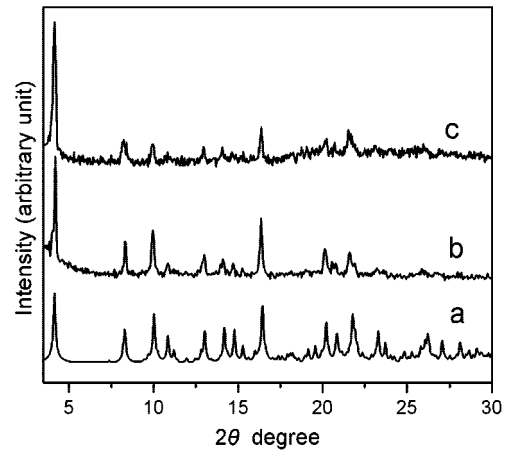

Figure 1. X-ray diffraction patterns (Cu Kα, λ = 1.5418 Å) of $TMPES \cdot 2AgBF_4 \cdot 3C_6H_6$ (**1**) and its apohost $TMPES \cdot 2AgBF_4$. (a) Calculated pattern from the single crystal structure of **1**; (b) observed from **1** at 298 K; (c) observed from the apohost at 298 K.

1-Trimethylsilylethynyl-4-methylthiobenzene. A Schlenk tube (100 mL) was loaded with a magnetic stirring bar, bis(triphenylphosphine)palladium(II) chloride (140.2 mg, 0.20 mmol), triphenylphosphine (280.4 mg, 1.07 mmol), copper(I) iodide (70.1 mg, 0.37 mmol), and 1-bromo-4-methylthiobenzene (2.03 g, 10.0 mmol). The Schlenk tube was then connected to a vacuum manifold, evacuated, and back-filled with nitrogen gas. After the Schlenk tube was thus purged three times, a 1:1 triethylamine/THF mixture (50.0 mL, prepurged with nitrogen gas) was injected via cannula under nitrogen protection, followed by injection of trimethylsilylacetylene (TMSA, 98%, 1.27 g, 13.0 mmol). The Schlenk tube was then sealed and stirred at 90 °C overnight (15 h). After being cooled to rt, the reaction mixture was poured into 200 mL of a 1:1 hexanes/dichloromethane mixture and then filtered through a silica gel plug. The solvents were then removed in vacuo and the dark yellow oily residue was purified by flash chromatography (silica gel, with hexane as the eluent) to provide a light yellow oily product (1.82 g, 83% based on 1-bromo-4-methylthiobenzene). ^1H NMR (300 MHz, $CDCl_3$): δ 0.18 (s, 9 H), 2.30 (s, 3H), 6.83 (d, 2H), 7.20 (d, 2H). ^{13}C NMR (75 MHz, $CDCl_3$): δ 0.10, 15.21, 94.10, 104.91, 119.43, 125.74, 132.22, 139.62.

4-Ethynyl-1-methylthiobenzene (EMTB). Tetrabutylammonium fluoride (TBAF, 1.0 M in THF, 1.54 mL) was injected into a two-neck round-bottom flask containing 1-trimethylsilylethynyl-4-methylthiobenzene (1.82 g, 8.3 mmol) in THF (30.0 mL) at rt with stirring. After being stirred for 1 h, the dark colored reaction mixture was passed through a silica gel plug, and the solvent was removed in vacuo to afford an orange oily product (1.22 g, 100%, based on 1-trimethylsilylethynyl-4-methylthiobenzene). ^1H NMR (300 MHz, $CDCl_3$): δ 2.56 (s, 3H), 3.80 (s, 1H), 7.24 (d, 2H), 7.27 (d, 2H). ^{13}C NMR (75 MHz, $CDCl_3$): δ 15.31, 76.80, 83.51, 118.32, 125.81, 132.42, 140.12.

Tetrakis[(4-methylthiophenyl)ethynyl]phenylsilane (TMPES). An *n*-butyllithium solution (1.6 M in hexane, 4.4 mL) diluted with THF (7.0 mL) was added dropwise to a THF solution (10.0 mL) of 4-ethynyl-1-methylthiobenzene (0.69 g, 4.7 mmol) at −78 °C under nitrogen protection. With the temperature maintained at −78 °C, a solution of anhydrous zinc chloride (0.96 g, 7.0 mmol) in THF (3.0 mL) was then added dropwise. The resulting mixture was then slowly warmed to rt. Under N_2 protection, the solution of the Cl−Zn-methylthiophenylacetylide was transferred via cannula into a degassed Schlenk tube that was previously loaded with

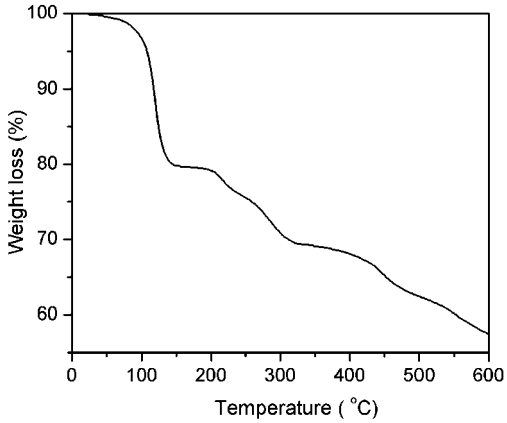

Figure 2. Thermogravimetric analysis plot for a solid sample of **1** in a He atmosphere.

tetrakis(4-bromophenyl)silane (0.61 g, 0.96 mmol), tetrakis(triphenylphosphine)palladium(0) (0.53 g, 0.46 mmol) and toluene (25.0 mL, prepurged with nitrogen gas). The Schlenk tube was then sealed and stirred at 120 °C for 2 days. After being cooled down to rt, the reaction solvents were removed in vacuo and the dark orange residue was purified by flash chromatography (silica gel, with 1:1 hexane/dichloromethane as the eluent) to provide a light yellow solid product (0.40 g, 47% yield based on tetrakis(4-bromophenyl)silane). ^{1}H NMR (300 MHz, $CDCl_3$): δ 2.51 (s, 12H), 7.21 (d, 8H), 7.45 (d, 8H), 7.54 (s, 16H). ^{13}C NMR (75 MHz, $CDCl_3$): δ 15.60, 89.54, 90.90, 119.54, 125.19, 126.09, 131.19, 132.18, 133.70, 136.41, 139.88.

X-ray Quality Single-Crystals of TMPES·$AgBF_4$·$3C_6H_6$ (1). A nitrobenzene (NB) solution (4.0 mL) of TMPES (24.0 mg, 26.0 mmol) was mixed with an NB solution (2.0 mL) of $AgBF_4$ (5.1 mg, 26 mmol) in a vial and the mixture was filtered to give a light yellow solution. The filtrate (held in a loosely capped vial) was then placed into a larger vial containing about 10 mL of benzene, with care taken to prevent direct contact of the filtrate and the benzene. The larger vial was then sealed and placed in a dark, quiet place for the vapor transport experiment. Clear, plate-like single crystals (20.0 mg, 72.0%, based on TMPES) suitable for X-ray data collection were formed over a period of about 7 days. X-ray powder diffraction of the product indicated a single phase consistent with the single-crystal structure (Figure 1). Elemental analysis calcd (%) for TMPES·$AgBF_4$·$3C_6H_6$: C, 69.38; H, 4.63. Found: C, 69.05; H, 4.61. This composition is also supported by the TGA measurement (see Figure 2).

Sorption Test on 1. The desolvated solid, which was obtained by drying the crystals under a vacuum at 120 °C for 30 min, exhibits poor solubility in many aromatic solvents (e.g., in those listed below in the vapor diffusion experiments). A small vial containing about 10 mg of the desolvated solid was placed into a larger vial containing about 10 mL of benzene, with care being taken to avoid direct contact of the solid sample and the liquid. The larger vial was then sealed for the vapor sorption experiment for a period of 3 or 4 days. To remove solvent fortuitously located on the exterior of the solid sample, *n*-hexane was then used to wash the crystals repeatedly (i.e., 3 × 3 mL), and the washed crystals were left in the air to dry off the hexane before elemental and solution ^{1}H NMR (300 MHz, DMSO-d_6/$CDCl_3$ = 1:1) analyses were carried out to test the presence and amount of guest included. Diffusion tests with other guests (e.g., *n*-hexane, toluene, hexafluorobenzene, anisole, chlorobenzene, 1,3-dichlorobenzene, 1-bromo-4-fluorobenzene, 4-bromo-1,2-difluorobenzene, anisole, ethylbenzene, and xylenes) were carried out in a similar setup. Elemental analysis calcd (%) for TMPES·$AgBF_4$: C, 64.57; H, 3.97. Found: C, 64.17; H, 4.16.

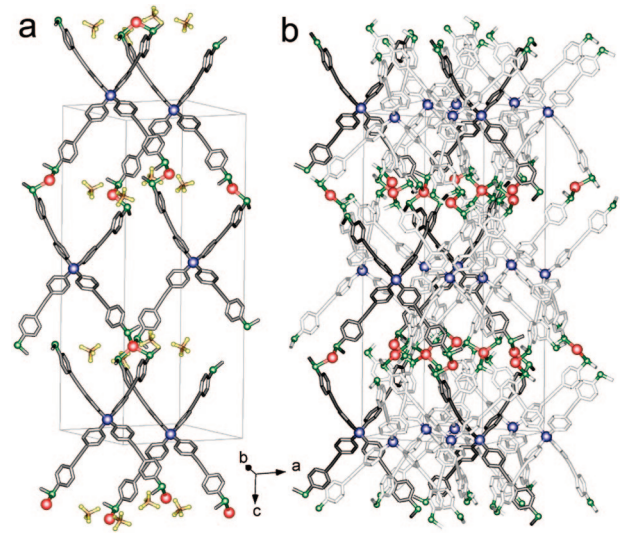

Figure 3. Crystal structure of **1**. (a) Diamondoid net with the BF_4^- anions; (b) four-interpenetrated nets (BF_4^- anions removed for clarity). Red sphere, Ag; green sphere, S; blue sphere, N; gray, C; yellow, BF_4.

TMPES·$AgBF_4$·C_6H_6: C, 66.38; H, 4.22. Found: C, 66.08; H, 4.39. TMPES·$AgBF_4$·$C_6H_5CH_3$: C, 66.61; H, 4.34. Found: C, 65.57; H, 3.96. TMPES·$AgBF_4$·C_6H_5Cl: C, 64.52; H, 4.02. Found: C, 63.95; H, 3.93. TMPES·$AgBF_4$·$C_6H_5NO_2$: C, 63.97; H, 3.99; N, 1.13. Found: C, 63.59; H, 3.73; N, 1.15. TMPES·$AgBF_4$·C_6H_4FBr: C, 61.40; H, 3.75. Found: C, 61.37; H, 3.77. TMPES·$AgBF_4$·$C_6H_5OCH_3$: C, 65.74; H, 4.28. Found: C, 65.28; H, 4.03. TMPES·$AgBF_4$·$C_6H_5CH_2CH_3$: C, 66.83; H, 4.45. Found: C, 66.41; H, 4.29.

Simulations. The Grand Canonical Monte Carlo (GCMC) simulations were carried out on helium (1 K, 1 kpa) and benzene (298 K, 101 kpa) using the guest-free crystal structure of **1**. A simulation cell of ~35−40 Å in each dimension was used in the calculations, which consists of 2, 2, and 1 unit cell length along the *a*-, *b*-, and *c*-axes, respectively (4 unit cells of **1**). In all three dimensions, periodic boundary conditions were applied. A typical length of GCMC simulation is composed of 1×10^7 steps. Burchart universal force field was employed in the simulations.

Results and Discussions

Single Crystal Structure of 1. Single-crystal samples of **1** were grown by diffusing benzene vapor into a nitrobenzene solution of TMPES and $AgBF_4$-interestingly, only benzene molecules are incorporated into the crystals thus formed. The asymmetric unit (space group *Pbca*) contains one TMPES molecule, one $AgBF_4$ unit and three benzene guests (i.e., TMPES·$AgBF_4$·$3C_6H_6$). The tetrapod molecule TMPES and the tetrahedral Ag(I) center (S−Ag distances, 2.567−2.591 Å; S−Ag−S angles, 104.2−113.5°) builds up an open-structure diamondoid network (Figure 3). The majority of the space is filled up via a 4-fold interpenetration of the individual diamondoid nets (and the associated BF_4 anions), whereas the remaining empty space (29.4% of the unit cell volume, i.e., the solvent-accessible domains calculated with the PLATON program[27]) was occupied by the benzene guests. The individual diamondoid nets are aligned such that the Ag^+ cations and the BF_4^- anions are concentrated in layer-like regions along the *bc* plane of the crystal structure

(27) Spek, A. L. *PLATON, A Multipurpose Crystallographic Tool*; Utrecht University: Utrecht, The Netherlands, 2001.

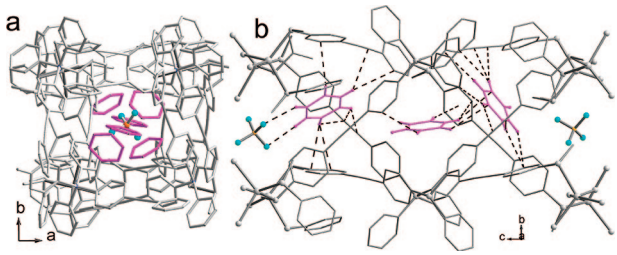

Figure 4. (a) Channel in **1** filled with benzene and BF_4 anion viewed along the *c* axis; (b) the arrangement of the benzene molecules and BF_4^- anions in the channel viewed along the *a* axis; the dotted lines represent the C−H···C and C−H···F hydrogen bonds (distance < 3.2 Å) in **1**. Purple, guest molecules; sky blue sphere, F; orange sphere, B; gray, the TMPES·$AgBF_4$ framework.

(Figure 3). The lamellar regions are quite flat, suggesting a microphase separation between the ionic domain and the organic domain in the structure.[28]

Compared with a cubic diamond structure, the network of **1** is elongated along one of the 4-fold helix directions (i.e., along the *c* axis, the pitch of the helix is 42.63 Å). The other two 4-fold helices (along 110 and 1−10, respectively) both have a pitch of 24.97 Å. The packing of the four individual nets results in distinct tube-like channels along the *c* axis (see Figure S1 in the Supporting Information). Each channel features a 2_1 screw axis at its center and four helices (one from each individual net) of the same handedness in the wall region; the individual tube thus formed is chiral. As in the prototypical diamond structure, the helix-based tubes are organized in a rectangular array, with each tube surrounded by four edge-sharing neighbors that have opposite chiralities, whereas the two corner-sharing neighboring tubes have the same chirality.

Moreover, the BF_4 anions are equally spaced in the channels (21.32 Å apart), dividing the channels into isolated cavities and further sequestering the benzene molecules. Each cavity houses three benzene molecules, which fit snugly inside and are crystallographically well-ordered, forming extensive van der Waals contacts (see Figure 4). The benzene molecules thus effectively take up the free space in the host networks (the solvent-accessible space in the benzene-filled structure of **1** is nearly zero, as is calculated with the PLATON program[27]). A molecular simulation[29] on the "neck region" (the smallest opening) of the channel along the *c* axis reveals two narrow openings within each isolated cavity between the two neighboring BF_4 (shown as tetrahedra in Figure S2 of the Supporting Information). The dimensions of these two neck regions are estimated as 2.3 and 2.1 Å, respectively, measured from center to center of the two He atoms (top of Figure S2 in the Supporting Information). Using 1.4 Å as the helium VDW radius,[30] the apertures are found to be 5.1 and 4.9 Å, respectively, both are decidedly smaller than the width of molecular benzene (6.1 Å). This clearly explains why the three benzene guests are well ordered in the structure under ambient conditions. In order to confirm this, we also performed a simulation on benzene. The simulated results match with the experimental data well

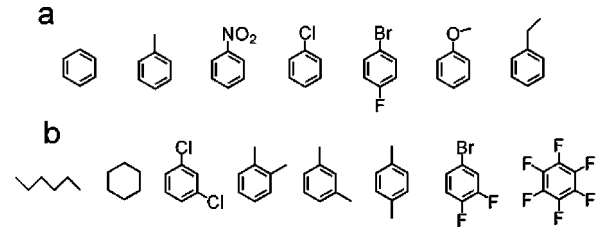

Figure 5. Molecules tested in the sorption experiments with the apohost (TMPES·$AgBF_4$): (a) guest molecules that were adsorbed by the apohost to form TMPES·$AgBF_4$·guest; (b) molecules that were not adsorbed by the apohost.

(see bottom of Figure S2 in the Supporting Information). Additionally, the sequestered state of the benzene guests is also reflected in the thermogravimetric analysis (TGA) plot of **1**, which features a steep weight loss of 18.47% at a temperature range (starting at 102.5 °C and finishing at 132.1 °C, see Figure 2) significantly higher than the boiling point of benzene (80 °C). The amount of weight loss is consistent with the formula of TMPES·$AgBF_4$·$3C_6H_6$ (calcd wt % for benzene: 17.35%).

Sorption Properties. In spite of their sequestered state as revealed in the single-crystal structure, the benzene guests can be removed (e.g., 30 min at 120 °C while being evacuated by a mechanical pump) without collapse of the host framework, as is shown in the X-ray powder diffraction studies (see pattern c in Figure 1). Notice that the powder patterns (ground sample pressed onto glass slide) in Figure S3 of the Supporting Information show strong orientation preference of the 001 face of the crystallites, with dominant 00n (n = even integers) series of reflections (see pattern b in Figure S3 of the Supporting Information), implying easy cleavage along the above-mentioned $AgBF_4$ layer in the structure (which might be attributed to the relatively weak Ag^+−thioether coordinating interaction). The evacuated solid sample of **1** was then subjected to sorption studies using a series of guest molecules (Figure 5) to further verify the structural integrity of the network and to probe the selectivity properties (note: no guest exchange was observed when as-made, benzene-filled crystallites of **1** were immersed in a guest solvent such as toluene for one week).

In the sorption study, the desolvated sample of **1** was placed above the guest solvents in a sealed container for vapor diffusion over (see Experimental Section for details). The solid samples thus treated were then dissolved in DMSO-d_6 and $CDCl_3$ for ^1H NMR measurements, which indicated that a saturated 1:1 TMPES/guest ratio was reached for the following: benzene, toluene, chlorobenzene, 1-bromo-4-fluorobenzene, anisole and nitrobenezene (Figure 5; see Figure S4 in the Supporting Information for the NMR spectra). Notice that the sorption tests here only partially recover the TMPES/guest ratio (the TMPES/benzene ratio is 3:1 in the pristine sample of **1**), indicating that the original TMPES/guest packing motif in **1** were not fully restored under these conditions. For ethylbenzene, the entry into the host network appears to be slower, taking over one week to reach the saturation host/guest ratio of 1:1. For the rest of guests (i.e., *n*-hexane, cyclohexane, 1,3-dichlorobenzene, hexafluorobenzene, 4-bromo-1,2-difluorobenzene, and *p*-xylenes), no entry into the host network was observed even

(28) Lee, S.; Mallik, A. B.; Xu, Z.; Lobkovsky, E. B.; Tran, L. *Acc. Chem. Res.* **2005**, *38*, 251.
(29) *Cerius2 Sorption Molecular Simulations*; Accelrys: San Diego, CA.
(30) Bondi, A. *J. Phys. Chem.* **1964**, *68*, 441.

after soaking the host solid in these solvents (neat) for more than half a month. X-ray powder diffraction studies on the guest-filled solid samples indicated that the structural integrity of host network was maintained after the uptake of the guest molecules (see Figure S3 in the Supporting Information).

In Figure 5, we grouped the molecules that were adsorbed and those that were not adsorbed by the apohost of **1** (TMPES·$AgBF_4$) under the above conditions. A most notable observation is that the adsorbed molecules consists of benzene, five monosubstituted and one para-substituted (i.e., 1-bromo-4-fluorobenzene) aromatic molecules. In other words, no meta- or ortho-substituted aromatics are allowed into the pores of **1**. This observation points to a rigorous selectivity toward the cross-sectional area of the aromatic guest: it appears that, to enter the pores, it is necessary for the guest to have the largest dimension in the cross-section (namely the width) being similar to that of benzene (6.1 Å). For clarity, we define the length-wise direction as being along the largest substituent and the benzenoid center, and the cross-section as being perpendicular to the length-wise direction.

The sensitivity to the cross-section of the guest is critical, even replacing the H atom with a fluorine atom (e.g., in C_6F_6) excludes the guest from entering the apohost net of **1**. In a separation experiment, the apohost of **1** (5.0 mg) was placed into a mixed solvent of 1:1 benzene/C_6F_6 (4.0 mL) for four days, and the apohost shows exclusive sorption of benzene (to form TMPES·$AgBF_4$·C_6H_6), without any observable amount of C_6F_6 (checked by ^9F solution NMR). As benzene and C_6F_6 have similar boiling points and tend to form cocrystals (making it difficulty to separate by distillation and crystallization), the unequivocal separation observed here suggests potential practical use.

The cases of *p*-xylene, 1-bromo-4-fluorobenzene (BrFBz) and ethylbenzene (EtBz) merit some attention. The cross-sections of all three molecules (with EtBz in the most stable staggered conformation) are the same as that of benzene, yet their sorption behaviors differ markedly: BrFBz enters normally like most of the group (a) molecules in Figure 5, EtBz as mentioned above, is sorbed more slowly and *p*-xylene is not sorbed at all. Such differences suggest that the structural features along the lengthwise direction of the guest molecules also become important for the longer molecules. Evidently a molecule much too long would not fit in the cavities of **1**. But the lengths for these three molecules (BrFBz, 9.32; *p*-xylene, 8.89; EtBz, 8.78−9.17 Å, depending on the Et- conformation) do not offer an intuitive correlation with the sorption behaviors, indicating that other aspects (e.g., polarity and shape) along the lengthwise direction might also influence the sorption properties. Further studies are necessary for a more in-depth understanding in this connection.

The sequestered state of guest molecules and the sorption activity points to substantial cooperative motion of the networks of **1** in the sorption process, which could be attributed to the structural flexibility of the network. It seems plausible that the individual nets in **1** may slide over one another cooperatively to allow the guest transport to occur.

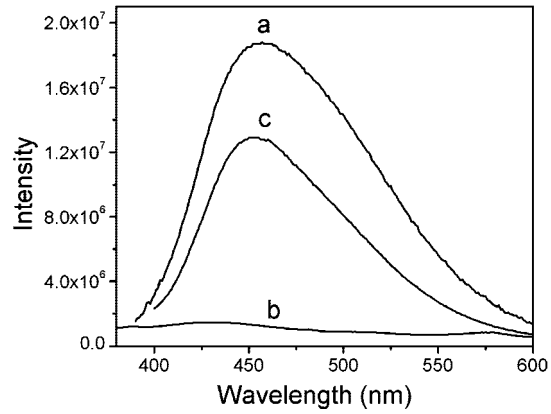

Figure 6. Illustration of the quenching effect of the nitrobenzene guest using room-temperature solid-state emission spectra (excitation wavelength λ_{ex} = 360 nm) of (a) an apohost (TMPES·$AgBF_4$) from evacuating on a pristine sample of **1**; (b) a host−guest sample (TMPES·$AgBF_4$·$C_6H_5NO_2$) from treating (a) with nitrobenzene vapor; (c) the recovered apohost (TMPES·$AgBF_4$) from evacuating on (b). No further reduction of intensity was observed in subsequent rounds of sorption−desorption cycles.

Examples of aperture-opening in host networks to allow sequestered molecules to escape are quite common,[6,11,13,31−36] and we suspect that, in the present case, the long and slender phenylalkynyl branches in the TMPES building block might contribute to the structural flexibility of the resultant network.

Fluorescence/Sensing Properties. The large aromatic π-electron system of molecule TMPES imparts significant fluorescence to the coordination network of **1**, both in the as-prepared sample (TMPES·$AgBF_4$·$3C_6H_6$) and the apohost (i.e., the evacuated sample TMPES·$AgBF_4$). The emission peak is around 450 nm, corresponding to a distinct blue color. As shown in Figure S5 of the Supporting Information, the entry of the above-mentioned guest molecules into the host net generally does not greatly affect the fluorescence intensity (peaks remain at 425−450 nm), with the only exception being nitrobenzene, which effectively suppresses the fluorescence emission. Fluorescence quenching of nitrobenzene on aromatic fluorophores is well-documented and is generally considered to involve a charge transfer from the fluorophore excited state to the low-lying molecular orbital associated with the strongly electron-withdrawing nitro group.[37,38]

The luminescence was effectively quenched by placing the desolvated solid of **1** (5.0 mg, crystallites as obtained from crystal growth, not ground) into the NB vapor for 4 days, as is demonstrated in both the fluorescence spectra (Figure 6) and visual observation (see Figure 7; after 2 days, the fluorescence was still visible under 254 nm UV radiation). To investigate the possible application of **1** as a sensor for

(31) Cussen, E. J.; Claridge, J. B.; Rosseinsky, M. J.; Kepert, C. J. *J. Am. Chem. Soc.* **2002**, *124*, 9574.
(32) Zhao, X.; Xiao, B.; Fletcher, A. J.; Thomas, K. M.; Bradshaw, D.; Rosseinsky, M. J. *Science* **2004**, *306*, 1012.
(33) Takamizawa, S.; Kohbara, M.-a. *Dalton Trans.* **2007**, 3640.
(34) Atwood, J. L.; Barbour, L. J.; Jerga, A.; Schottel, B. L. *Science* **2002**, *298*, 1000.
(35) Barbour, L. J. *Chem. Commun.* **2006**, 1163.
(36) Dobrzanska, L.; Lloyd, G. O.; Raubenheimer, H. G.; Barbour, L. J. *J. Am. Chem. Soc.* **2006**, *128*, 698.
(37) Sanchez, J. C.; DiPasquale, A. G.; Rheingold, A. L.; Trogler, W. C. *Chem. Mater.* **2007**, *19*, 6459.
(38) Lewis, F. D.; Daublain, P.; Delos Santos, G. B.; Liu, W.; Asatryan, A. M.; Markarian, S. A.; Fiebig, T.; Raytchev, M.; Wang, Q. *J. Am. Chem. Soc.* **2006**, *128*, 4792.

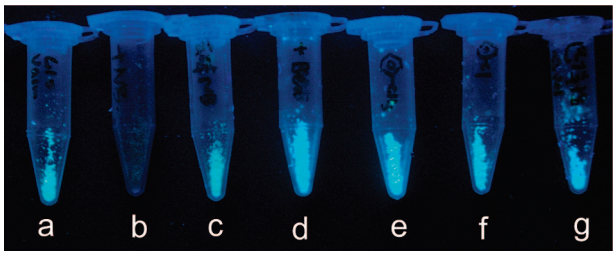

Figure 7. Photograph of the UV-irradiated (254 nm) solid samples derived from **1** under different evacuation/sorption conditions: (a) an apohost (TMPES·$AgBF_4$) from evacuating on a pristine sample of **1**; (b) a nitrobenzene-filled sample (TMPES·$AgBF_4$·$C_6H_5NO_2$) from treating (a) with nitrobenzene vapor; (c) the recovered apohost (TMPES·$AgBF_4$) from evacuating on (b); (d) a benzene-filled sample (TMPES·$AgBF_4$·C_6H_6); (e) a toluene-filled sample (TMPES·$AgBF_4$·C_7H_8); (f) a chlorobenzene-filled sample (TMPES·$AgBF_4$·C_6H_5Cl); (g) a 1-bromo-4-fluorobenzene-filled sample (TMPES·$AgBF_4$·C_6H_4BrF). Samples d−g were prepared similarly to that of (b).

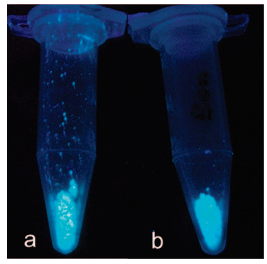

Figure 8. Photograph taken under a UV lamp (254 nm) of (a) a pristine solid sample of the TMPES molecule and (b) a solid sample of TMPES bathed in nitrobenzene vapor for four days.

nitrobenzene, the sorption/desorption cycle was tested with nitrobenzene vapor (sorption procedure being the same as before). As shown in spectrum b of Figure 6, the fluorescence substantially recovers upon evacuating the NB molecules from the nitrobenzene-filled sample (by pumping at 140 °C for 2 h; removal of nitrobenzene molecules was confirmed by solution ^{1}H NMR). The sorption/desorption process can be cycled without affecting the structural integrity or the overall photoluminescence features of the host net (see Figure 6 for the fluorescence). Grinding the crystallites of **1** in fine powders greatly speeds up the fluorescent response; in fact, the fluorescence of the ground powder completely disappears under UV light within 3 h of immersion in nitrobenzene vapor. Even faster response might be achieved with more dispersed and finer particles of **1** (e.g., in the form of a thin film). Further study on the processing of the crystallites of **1** for this purpose appears worthwhile to pursue.

How does the organic compound TMPES differ from the network system of **1** in the sensing of nitrobenzene? For this, a powder sample of the TMPES molecule was placed in nitrobenzene vapor under the same conditions as for **1** (for 5 days at room temperature). The fluorescence of the TMPES powder remains visually unchanged under UV radiation (Figure 8). No presence of nitrobenzene was detected in the TMPES powder sample (from weight monitoring, IR, and ^{1}H solution NMR) after the sample was bathed in the nitrobenzene vapor, indicating that nitrobenzene molecules did not impregnate the TMPES powder sample. This comparative experiment highlights the crucial role of the open-framework features of **1** in providing for the sensing and sorption properties.

Table 1. X-ray Crystallographic Data for 1

	1
chem formula	$C_{78}H_{62}S_4AgBF_4Si$
fw	1350.29
space group	*Pbca*
a (Å)	17.659 (2)
b (Å)	17.648 (2)
c (Å)	42.628 (4)
V (Å^3)	13285 (2)
Z	8
ρ_{calcd} (g/cm^3)	1.350
wavelength (Å)	0.71073 (Mo Kα)
abs coeff (μ) (cm^{-1})	5.03
$R_1{}^a$	7.25% [$I > 2\sigma(I)$]
$wR_2{}^b$	19.13% [$I > 2\sigma(I)$]

^{a} $R_1 = \sum||F|_o - |F_c||/\sum|F_o|$. ^{b} $wR_2 = \{\sum[w(F_o^2 - F_c^2)^2]/\sum[w(F_o^2)^2]\}^{1/2}$.

Taken together, the remarkable selectivity for small aromatics observed for **1** originates from two major features: (1) the extensive interpenetration of the individual diamondoid nets and the benzene guests that are snugly enclathrated, and thus template the shape and size of the resultant cavities; (2) the network flexibility that allows for the passage of guest molecules in and out of the isolated cavities in **1**. Although the inclusion of the benzene molecules appears to be largely fortuitous at this stage (and it remains unclear why the cosolvent nitrobenzene was not incorporated), the long and slender phenylalkynyl branches of the TMPES molecule primes the extensive interpenetration of the individual nets and might contribute to the network flexibility associated with guest exchange process. In future studies, one might use different solvent systems for growing the host net, so as to modify size and shape of the cavities. For example, using ortho- or meta-substituted dichlorobenzene or hexafluorobenzene might contribute to cavities that allow for the exchange of aromatic guests larger than the ones observed here with **1**. Also, the methyl group in TMPES could be replaced by a phenyl or 4-methoxyphenyl group, so as to influence the degree of interpenetration as well as the size and shape of the cavities within the prospective coordination networks.

Acknowledgment. This work is supported by a grant from the Research Grants Council of the Hong Kong Special Administrative Region, China (Project 9041212 (CityU 103407)). The diffractometer was funded by NSF Grant 0087210, by the Ohio Board of Regents Grant CAP-491, and by YSU.

Supporting Information Available: Full crystallographic data in CIF format for compounds **1**. X-ray powder diffraction patterns and room-temperature solid-state emission spectra for bulk samples of **1**, the apohost, and the guest-exchanged samples (PDF). This material is available free of charge via the Internet at http://pubs.acs.org.

CM8027687